Scale Spaces on the 3D Euclidean Motion Group for Enhancement of HARDI Data

Erik Franken[1] and Remco Duits[1,2]

[1] Department of Biomedical Engineering
[2] Department of Mathematics and Computer science,
Eindhoven University of Technology, The Netherlands
{E.M.Franken,R.Duits}@tue.nl

Abstract. In previous work we studied left-invariant diffusion on the 2D Euclidean motion group for crossing-preserving coherence-enhancing diffusion on 2D images. In this paper we study the equivalent three-dimensional case. This is particularly useful for processing High Angular Resolution Diffusion Imaging (HARDI) data, which can be considered as 3D orientation scores directly. A complicating factor in 3D is that all practical 3D orientation scores are functions on a coset space of the 3D Euclidean motion group instead of on the entire group. We show that, conceptually, we can still apply operations on the entire group by requiring the operations to be α-*right-invariant*. Subsequently, we propose to describe the local structure of the 3D orientation score using left-invariant derivatives and we smooth 3D orientation scores using left-invariant diffusion. Finally, we show a number of results for linear diffusion on artificial HARDI data.

1 Introduction

A common approach for enhancing elongated structures in noisy images is by nonlinear anisotropic diffusion on the image [1]. This can be regarded as calculating a nonlinear scale space on the additive group $(\mathbb{R}^n, +)$, i.e. the translation group. In our earlier work [2, 3, 5], we proposed to enhance elongated structures *via* the *orientation score* of a 2D image, which has the practical advantage that crossing structures can be handled appropriately. An orientation score of a 2D image is a function on the 2D Euclidean motion group $SE(2)$, which is constructed from a 2D image using an invertible transformation. The image enhancement in our previous work is accomplished by a nonlinear diffusion process in the orientation score of the image (which is a 3D dataset: 2 spatial dimensions and 1 orientation dimension), followed by an inverse orientation score transformation to obtain an enhanced image.

In this paper we go one step further and investigate how we can apply the same techniques to 3D orientation scores. Such orientation score is a 5D dataset, i.e. 3 spatial dimensions and 2 orientation dimensions. The 3D case is very relevant for many (bio)medical problems, since many (bio)medical images are intrinsically 3D. Our main application of interest is *high angular resolution diffusion imaging* (HARDI).

X.-C. Tai et al. (Eds.): SSVM 2009, LNCS 5567, pp. 820–831, 2009.

With the term HARDI we refer to all diffusion MRI techniques, in which the diffusion profile on each spatial position is modeled by a *function on the sphere*, which provides richer information especially in regions where different fibrous structures cross or bifurcate [4,6,7,8]. Roughly speaking the MRI scanner measures the probability of finding a water molecule at each position for a certain direction, where the number of acquired directions can be varied. Clearly, all data obtained using any HARDI technique can be considered as 3D orientation scores *directly*.

Remarkably, in HARDI processing algorithms that are proposed in literature, the data is processed as function on the sphere for each spatial position separately, see e.g. [4, 7, 9]. In our approach, we consider both the spatial and the orientational part to be included in the *domain*, so a HARDI dataset is considered as a function $\mathbb{R}^3 \rtimes S^2 \to \mathbb{R}$. Furthermore, we explicitly employ the proper underlying group structure. The advantage is that we can enhance the data using both orientational and spatial neighborhood information, which potentially leads to improved enhancement and detection algorithms.

3D orientation scores are defined as functions $u : \mathbb{R}^3 \rtimes S^2 \to \mathbb{R}$ or $\mathbb{C}$, where $\mathbb{R}^3$ is the spatial domain and $S^2 = \{\boldsymbol{n} \in \mathbb{R}^3 \,|\, \|\boldsymbol{n}\| = 1\}$ is the domain of a unit sphere. In this paper, the domain of u is parameterized by $(\boldsymbol{x}, \boldsymbol{n})$, where $\boldsymbol{x} = (x, y, z) \in \mathbb{R}^3$ and $\boldsymbol{n} \in S^2$. Figure 1(a) shows an example clarifying the structure of a 3D orientation score.

This paper will start with the introduction of the group structure of the 3D orientation score domain, i.e. the 3D Euclidean motion group $SE(3)$. Subsequently, we will introduce the important differential geometry on $SE(3)$, needed

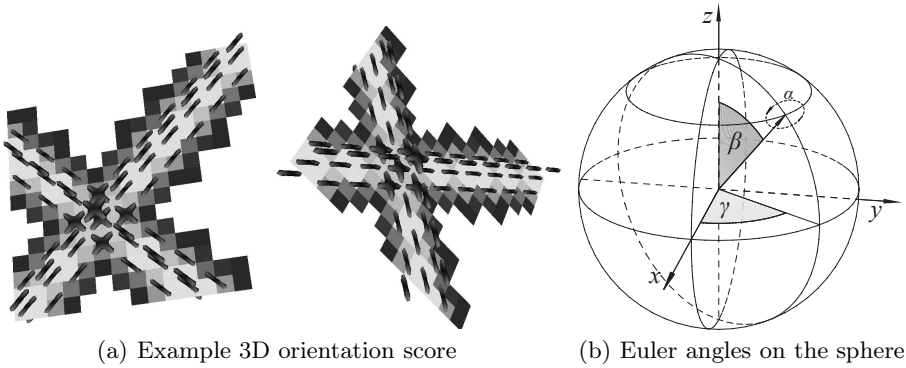

(a) Example 3D orientation score (b) Euler angles on the sphere

Fig. 1. (a) Visualization of a simple 3D orientation score $u(\boldsymbol{x}, \boldsymbol{n})$ containing two crossing straight lines, visualized using Q-ball glyphs in the DTI tool (see http://www.bmia.bmt.tue.nl/software/dtitool/) from two different viewpoints. At each (relevant) spatial position $\boldsymbol{x}$ the function on the sphere $u(\boldsymbol{x}, \cdot)$ is displayed by a so-called *glyph*, which is given by $\boldsymbol{n} \mapsto \boldsymbol{x} + q\, u(\boldsymbol{x}, \boldsymbol{n})\boldsymbol{n}$ where q is a scaling factor. (b) Intuition of coset space $SO(3)/SO(2)$: the Euler angles (α, β, γ) are needed to parametrize rotation in $SO(3)$, while the two angles (β, γ) are sufficient to describe positions on the unit sphere, represented by a unit vector. The third Euler angle α is in fact a rotation of this vector around its own axis, leaving the vector invariant. Thus, each position on the sphere is identified by a coset space $SO(3)/SO(2)$ cf. (4).

to estimate tangent vectors that locally fit best to the elongated structures in the 3D orientation score. The next topic will be the diffusion on 3D orientation scores, which yields a scale space representation of the $SE(3)$ group. The paper will end with results of linear $SE(3)$-diffusion on artificial HARDI datasets.

2 Group Structure of the Domain of 3D Orientation Scores

2.1 The Rotation Group $SO(3)$ and Coset Space $SO(3)/SO(2)$

The noncommutative group of 3D rotations is defined as matrix group by

$$SO(3) = \{\mathbf{R} \,|\, \mathbf{R} \in \mathbb{R}^{3\times 3}, \mathbf{R}^{\mathrm{T}} = \mathbf{R}^{-1}, \det(\mathbf{R}) = 1\}. \tag{1}$$

In this section, we will first consider different parameterizations of $SO(3)$. Then, we will describe the coset space $SO(3)/SO(2)$, which is an essential prerequisite to relate functions on the sphere (i.e. two angles) to functions on $SO(3)$ (i.e. three angles).

The relation between positions on the sphere S^2 and a 3D rotation $SO(3)$ is established by rotating the vector $\boldsymbol{e}_z$, i.e.

$$\boldsymbol{n} = \mathbf{R} \cdot \boldsymbol{e}_z. \tag{2}$$

This relation shows that the resulting position $\boldsymbol{n}$ on the sphere is independent on an arbitrary rotation around the z-axis, that is $\mathbf{R}\,\mathbf{R}_\alpha^{\boldsymbol{e}_z} \cdot \boldsymbol{e}_z = \mathbf{R} \cdot \boldsymbol{e}_z$ for all α, where $\mathbf{R}_\alpha^{\boldsymbol{n}}$ denotes rotation over α around the axis defined by vector $\boldsymbol{n}$. This means that a function on the sphere is not equivalent to a function on the complete rotation group $SO(3)$, but rather a function on the set that partitions $SO(3)$ into *left cosets* $SO(3)/\mathrm{stab}(\boldsymbol{e}_z)$ where $\mathrm{stab}(\boldsymbol{e}_z)$ denotes the subgroup of $SO(3)$ of all rotations around the z-axis, as is made intuitive in Figure 1(b).

A left coset $[g]_H$ of a group G with subgroup H is defined as the set

$$[g]_H = gH = \{gh | h \in H\}, \tag{3}$$

for any $g \in G$. The left cosets form a partition of the group, i.e. the group is divided into disjoint cosets, and the set of all of these cosets is denoted by G/H. Two group elements $g_1 \in G$ and $g_2 \in G$ have an equivalence relation $g_1 \sim g_2$ if they belong to the same left coset, i.e. $g_1 H = g_2 H$.

In the case $SO(3)/\mathrm{stab}(\boldsymbol{e}_z)$, we have the equivalence relation $\mathbf{R}_1 \sim \mathbf{R}_2$ iff there is an α such that $\mathbf{R}_1 \mathbf{R}_\alpha^{\boldsymbol{e}_z} = \mathbf{R}_2$. From now on we will write $SO(3)/SO(2)$ rather than $SO(3)/\mathrm{stab}(\boldsymbol{e}_z)$ since $\mathrm{stab}(\boldsymbol{e}_z)$ and $SO(2)$ are isomorphic. The cosets $SO(3)/SO(2)$ are isomorphic to the space of the unit vectors of (2), i.e.

$$SO(3)/SO(2) \cong S^2 = \big\{\boldsymbol{n} \in \mathbb{R}^3 \big| \|\boldsymbol{n}\| = 1\big\}. \tag{4}$$

The isomorphism is given by means of (2). The set of all the cosets $SO(3)/SO(2)$ can be parameterized using only two angles rather than three angles, for instance as $[\mathbf{R}_\gamma^{\boldsymbol{e}_z} \mathbf{R}_\beta^{\boldsymbol{e}_y}]_{SO(2)} \in SO(3)/SO(2)$ and therefore $\boldsymbol{n}(\beta,\gamma) = \mathbf{R}_\gamma^{\boldsymbol{e}_z} \mathbf{R}_\beta^{\boldsymbol{e}_y} \boldsymbol{e}_z \in S^2$. Note that the set of all disjoint cosets $SO(3)/SO(2)$ does *not* form a group since $SO(2)$ is not a normal subgroup of $SO(2)$, so $[g_1]_{SO(2)}\,[g_2]_{SO(2)} \neq [g_1 g_2]_{SO(2)}$.

2.2 The 3D Euclidean Motion Group $SE(3)$

The *3D Euclidean motion group* is the group of 3D translations and 3D rotations, i.e. $SE(3) = \mathbb{R}^3 \rtimes SO(3)$. An element of $SE(3)$ can be parameterized by $(\boldsymbol{x}, \mathbf{R})$ where $\boldsymbol{x} \in \mathbb{R}^3$ is the translation vector and $\mathbf{R} \in SO(3)$ is the rotation matrix. The group product and inverse of $SE(3)$ are given by

$$\begin{aligned} g\,g' &= (\boldsymbol{x}, \mathbf{R})\,(\boldsymbol{x}', \mathbf{R}') = (\boldsymbol{x} + \mathbf{R}\cdot\boldsymbol{x}', \mathbf{R}\cdot\mathbf{R}'), \\ g^{-1} &= (\boldsymbol{x}, \mathbf{R})^{-1} = (-\mathbf{R}^{-1}\boldsymbol{x}, \mathbf{R}^{-1}). \end{aligned} \tag{5}$$

To map the structure of a group to operators on orientation scores, we need a *representation*. A representation is a mapping of the form $\mathcal{R} : G \to \mathcal{B}(H)$, where H is the linear space of orientation scores and $\mathcal{B}(H)$ is the space of bounded linear invertible operators $H \to H$, that maps a group element to an operator where the group properties are preserved, i.e. $\mathcal{R}_g\mathcal{R}_h = \mathcal{R}_{gh}$ and $\mathcal{R}_e = \mathcal{I}$. On $SE(3)$ we define the *left-* and *right-regular representations* on a function $U \in \mathbb{L}_2(\mathrm{SE}(3))$ as

$$(\mathcal{L}_g \circ U)(h) = U(g^{-1}h), \quad g, h \in SE(3), \tag{6}$$

$$(\mathcal{Q}_g \circ U)(h) = U(h\,g), \qquad g, h \in SE(3). \tag{7}$$

The matrix *Lie algebra* [10] $T_e(SE(3))$ is spanned by the following basis

$$\begin{aligned} \mathbf{X}_1 &= \begin{pmatrix} 0&0&0&1\\ 0&0&0&0\\ 0&0&0&0\\ 0&0&0&0 \end{pmatrix}, \qquad \mathbf{X}_2 = \begin{pmatrix} 0&0&0&0\\ 0&0&0&1\\ 0&0&0&0\\ 0&0&0&0 \end{pmatrix}, \qquad \mathbf{X}_3 = \begin{pmatrix} 0&0&0&0\\ 0&0&0&0\\ 0&0&0&1\\ 0&0&0&0 \end{pmatrix}, \\ \mathbf{X}_4 &= \begin{pmatrix} 0&0&0&0\\ 0&0&-1&0\\ 0&1&0&0\\ 0&0&0&0 \end{pmatrix}, \qquad \mathbf{X}_5 = \begin{pmatrix} 0&0&1&0\\ 0&0&0&0\\ -1&0&0&0\\ 0&0&0&0 \end{pmatrix}, \qquad \mathbf{X}_6 = \begin{pmatrix} 0&-1&0&0\\ 1&0&0&0\\ 0&0&0&0\\ 0&0&0&0 \end{pmatrix}. \end{aligned} \tag{8}$$

The nonzero commutators can be found by $[\mathbf{X}_i, \mathbf{X}_j] = \mathbf{X}_i\mathbf{X}_j - \mathbf{X}_j\mathbf{X}_i$.

By calculating the matrix exponents we find the following matrix representation of the $SE(3)$ group

$$\begin{aligned} \mathbf{E}_{(\boldsymbol{x},\mathbf{R})} &= \exp(x\,\mathbf{X}_1 + y\,\mathbf{X}_2 + z\,\mathbf{X}_3)\,\exp(\check{\gamma}\,\mathbf{X}_4)\,\exp(\check{\beta}\,\mathbf{X}_5)\,\exp(\check{\alpha}\,\mathbf{X}_6) \\ &= \begin{pmatrix} \mathbf{R} & \boldsymbol{x} \\ \mathbf{0} & 1 \end{pmatrix}, \qquad \text{with } \mathbf{R} = \mathbf{R}_{\check{\gamma}}^{\boldsymbol{e}_x}\mathbf{R}_{\check{\beta}}^{\boldsymbol{e}_y}\mathbf{R}_{\check{\alpha}}^{\boldsymbol{e}_z}. \end{aligned} \tag{9}$$

where $(\check{\alpha}, \check{\beta}, \check{\gamma})$ is a possible Euler angle parametrization of the rotation group $SO(3)$, see [5, Chapter 7].

2.3 Left-Invariance and Right-Invariance

An operator $\Phi : \mathbb{L}_2(SE(3)) \to \mathbb{L}_2(SE(3))$ is left-invariant if it commutes with the left-regular representation (6)

$$\forall\ g \in SE(3) : \mathcal{L}_g \circ \Phi = \Phi \circ \mathcal{L}_g, \tag{10}$$

and similarly an operator Φ is right-invariant if it commutes with the right-regular representation (7)

$$\forall\ g \in SE(3) : \mathcal{Q}_g \circ \Phi = \Phi \circ \mathcal{Q}_g. \tag{11}$$

In this work we aim at *left-invariant* operations and consider right-invariant operations senseless. The rationale behing this will be clarified below. Define $\mathcal{W} : (SE(3) \to \mathbb{C}) \to (\mathbb{R}^3 \to \mathbb{C})$ to be the operator that calculates the *orientation-marginal*,

$$\mathcal{W}[U](\boldsymbol{x}) = \int_{SO(3)} U(\boldsymbol{x}, \mathbf{R}) \mathrm{d}\mu(\mathbf{R}). \tag{12}$$

where $\mathrm{d}\mu$ is the Haar measure, which is designed in order to fulfill requirement

$$\int_{SO(3)} F(\mathbf{R}) \mathrm{d}\mu(\mathbf{R}) = \int_{SO(3)} F(\mathbf{R} \cdot \mathbf{R}') \mathrm{d}\mu(\mathbf{R}), \quad \forall \mathbf{R}' \in SO(3). \tag{13}$$

It is easy to derive that for the left-regular representation

$$\mathcal{U}_g \circ \mathcal{W} \circ U = \mathcal{W} \circ \mathcal{L}_g \circ U,\ \forall g \in SE(3), \tag{14}$$

where $\mathcal{U}$ is a representation of $SE(3)$ on $\mathbb{L}_2(\mathbb{R}^3)$ defined by $(\mathcal{U}_{(\boldsymbol{x}', \mathbf{R}')} f)(\boldsymbol{x}) = f((\mathbf{R}')^{-1}(\boldsymbol{x} - \boldsymbol{x}'))$. On the other hand, we note that

$$(\mathcal{W} \circ \mathcal{Q}_{(\boldsymbol{x}, \mathbf{R})} \circ U)(\boldsymbol{x}', \mathbf{R}') = \int_{SO(3)} U(\boldsymbol{x}' + \mathbf{R}'\boldsymbol{x}, \mathbf{R}'\mathbf{R}) \mathrm{d}\mu(\mathbf{R}'), \tag{15}$$

which shows that the integral variable $\mathbf{R}'$ enters the spatial part, making it impossible to find a relation equivalent to (14) for the right-regular representation. In words, the left-regular representation "commutes" with $\mathcal{W}$, where $\mathcal{L}_g$ changes into $\mathcal{U}_g$ since the function space changes from $SE(3)$ to $\mathbb{R}^3$, while it is not possible to find such a relation for the right-regular representation. This observation makes it sensible to favor operators Φ to be left-invariant, i.e. $\mathcal{W} \circ \Phi \circ \mathcal{L}_g \circ U = \mathcal{W} \circ \mathcal{L}_g \circ \Phi \circ U = \mathcal{U}_g \circ \mathcal{W} \circ \Phi \circ U$ states that applying a group transformation ($\mathcal{L}_g$) on the input U renders the same result as applying the same group transformation ($\mathcal{U}_g$) on the orientation-marginal of the output.

2.4 Functions on $SE(3)$ and $\mathbb{R}^3 \rtimes S^2$

In the beginning of this paper we defined a 3D orientation score u as a function of three spatial variables and only two angular variables describing a position on the sphere. However, since the sphere S^2 is isomorphic to the coset space $SO(3)/SO(2)$, rather than the entire rotation group $SO(3)$, such an orientation score is not a function on the entire Euclidean motion group $SE(3)$, but rather a function on the coset space $SE(3)/(\mathbf{0} \times \mathrm{stab}(\mathbf{e}_z))$. Here, $(\mathbf{0} \times \mathrm{stab}(\mathbf{e}_z))$ denotes the $SE(2)$ subgroup of rotations around the z-axis and translation $\mathbf{0}$, which is isomorphic to $SO(2)$. Analogously to the isomorphism $SO(3)/SO(2) \cong S^2$, we have the isomorphism $SE(3)/(\mathbf{0} \times \mathrm{stab}(\mathbf{e}_z)) \cong \mathbb{R}^3 \rtimes S^2$.

For the analysis it is more convenient to consider functions on $\mathbb{R}^3 \rtimes S^2$ as functions on the entire group $SE(3)$ with the extra property of α-*right-invariance*. A function $\tilde{U} : SE(3) \to \mathbb{C}$ is defined to be α-*right-invariant* if

$$\begin{aligned} &\mathcal{Q}_{(\mathbf{0},\mathbf{R}_\alpha^{\boldsymbol{e}_z})} \circ \tilde{U} = \tilde{U}, \quad \forall\, \alpha, \text{ that is,} \\ &\tilde{U}(\boldsymbol{x}, \mathbf{R}\mathbf{R}_\alpha^{\boldsymbol{e}_z}) = \tilde{U}(\boldsymbol{x}, \mathbf{R}), \quad \forall\, \alpha, \end{aligned} \tag{16}$$

where we write $\tilde{U}$ rather than U to make explicit in the notation that the function is α-right-invariant. We observe that the value of $\tilde{U}(\boldsymbol{x}, \mathbf{R})$ is independent on a rotation of the z-axis applied on the right-side, so $\tilde{U}$ can be identified one-to-one to an orientation score $u : \mathbb{R}^3 \rtimes S^2 \to \mathbb{C}$, as

$$\tilde{U}(\boldsymbol{x}, \mathbf{R}) = u(\boldsymbol{x}, \mathbf{R} \cdot \boldsymbol{e}_z), \quad \text{where } \tilde{U} \text{ is } \alpha\text{-right-invariant.} \tag{17}$$

In this paper we will mostly work with the α-right-invariant function $\tilde{U}$, because it is more convenient to work with functions on the group.

2.5 $SE(3)$-Convolutions

It can be shown that all operations on orientation scores that are *linear* and *left-invariant*, can be expressed as an $SE(3)$-convolution, which is defined by

$$(\Psi \ *_{SE(3)} \ U)(g) = \int_{SE(3)} \Psi(h^{-1}g) U(h) dh. \tag{18}$$

More explicitly this yields

$$(\Psi *_{SE(3)} U)(\boldsymbol{x}, \mathbf{R}) = \int_{\mathbb{R}^3} \int_{SO(3)} \Psi(\mathbf{R}'^{-1}(\boldsymbol{x} - \boldsymbol{x}'), \mathbf{R}'^{-1}\,\mathbf{R}) U(\boldsymbol{x}', \mathbf{R}')\, \mathrm{d}\boldsymbol{x}\, \mathrm{d}\mu(\mathbf{R}'), \tag{19}$$

where $\mathrm{d}\mu(\mathbf{R}')$ is defined in (13).

For an α-right-invariant $\tilde{U}$ cf. (16) we need to put additional requirements on the kernel Ψ. We require the result $\Psi *_{SE(3)} \tilde{U}$ to be α-right-invariant as well, leading to the following requirement

$$\mathcal{Q}_{(\mathbf{0},\mathbf{R}_{\alpha'}^{\boldsymbol{e}_z})} \circ (\tilde{\Psi} *_{SE(3)} (\mathcal{Q}_{(\mathbf{0},\mathbf{R}_\alpha^{\boldsymbol{e}_z})} \circ \tilde{U})) = \tilde{\Psi} *_{SE(3)} \tilde{U}, \quad \forall\, \alpha, \alpha'. \tag{20}$$

This imposes requirements on the kernel $\tilde{\Psi}$. One can easily verify that the following properties hold for the $SE(3)$-convolution of (18)

$$\mathcal{Q}_g(\Psi *_{SE(3)} U) = (\mathcal{Q}_g \Psi) *_{SE(3)} U, \ \forall g \in SE(3), \tag{21}$$

$$(\mathcal{L}_g \Psi) *_{SE(3)} U = \Psi *_{SE(3)} (\mathcal{Q}_{g^{-1}} U), \ \forall g \in SE(3). \tag{22}$$

Using the latter two equations, the left-hand side of (20) can now be rewritten as

$$\begin{aligned} \mathcal{Q}_{(\mathbf{0},\mathbf{R}_{\alpha'}^{\boldsymbol{e}_z})} \circ (\tilde{\Psi} *_{SE(3)} (\mathcal{Q}_{(\mathbf{0},\mathbf{R}_\alpha^{\boldsymbol{e}_z})} \circ \tilde{U})) &= ((\mathcal{Q}_{(\mathbf{0},\mathbf{R}_{\alpha'}^{\boldsymbol{e}_z})} \circ \tilde{\Psi}) *_{SE(3)} (\mathcal{Q}_{(\mathbf{0},\mathbf{R}_\alpha^{\boldsymbol{e}_z})} \circ \tilde{U})) \\ &= (\mathcal{L}_{(\mathbf{0},\mathbf{R}_{-\alpha}^{\boldsymbol{e}_z})} \circ \mathcal{Q}_{(\mathbf{0},\mathbf{R}_{\alpha'}^{\boldsymbol{e}_z})} \circ \tilde{\Psi}) *_{SE(3)} \tilde{U}. \end{aligned} \tag{23}$$

Therefore

$$\tilde{\Psi} = \mathcal{L}_{(\mathbf{0},\mathbf{R}^{\boldsymbol{e}_z}_{-\alpha})} \circ \mathcal{Q}_{(\mathbf{0},\mathbf{R}^{\boldsymbol{e}_z}_{\alpha'})} \circ \tilde{\Psi}, \text{ for all } \alpha,\ \alpha', \tag{24}$$

so $\tilde{\Psi}$ is required to be both α-right-invariant and α-left-invariant (i.e. $\mathcal{L}_{(\mathbf{0},\mathbf{R}^{\boldsymbol{e}_z}_{\alpha'})} \circ \tilde{U} = \tilde{U}$ for all α'). More explicitly this yields

$$\tilde{\Psi}(\boldsymbol{x},\mathbf{R}) = \tilde{\Psi}((\mathbf{R}^{\boldsymbol{e}_z}_{\alpha})^{-1}\boldsymbol{x}, (\mathbf{R}^{\boldsymbol{e}_z}_{\alpha})^{-1}\mathbf{R}\mathbf{R}^{\boldsymbol{e}_z}_{\alpha'}), \text{ for all } \alpha,\ \alpha'. \tag{25}$$

3 Differential Geometry on $SE(3)$

In [3] we introduced the basic differential geometry on $SE(2)$. In this section we establish the same concepts for $SE(3)$. We will introduce the left-invariant vector fields and left-invariant derivatives, and a procedure to estimate tangent vectors that locally fit best to elongated structures in 3D orientation scores. A more extensive description, including explicit expression for e.g. curvature and torsion, can be found in [5, Chapter 7].

3.1 Left-Invariant Derivatives in $SE(3)$

Using the matrix representation cf. equation (9), left-invariant derivatives are given by

$$(\mathcal{A}_i U)(\mathbf{E}_g) = \lim_{h\to 0} \frac{U(\mathbf{E}_g \cdot \exp(h\,\mathbf{X}_i)) - U(\mathbf{E}_g)}{h}. \tag{26}$$

The tangent space of $g \in SE(3)$ is spanned by these vector fields, i.e. $T_g(SE(3)) = \text{span}\{\mathcal{A}_1\big|_g, \mathcal{A}_2\big|_g, \mathcal{A}_3\big|_g, \mathcal{A}_4\big|_g, \mathcal{A}_5\big|_g, \mathcal{A}_6\big|_g\}$ where we define $\left(\mathcal{A}_i\big|_g\right)(U) = (\mathcal{A}_i U)(\mathbf{E}_g)$. Left-invariant derivatives $\mathcal{A}_1$, $\mathcal{A}_2$,and $\mathcal{A}_3$ can be implemented simply by approximating (26) using finite differences.

On an α-right-invariant function $\tilde{U}$, $\mathcal{A}_3\tilde{U}(g)$ is always α-right-invariant since $\exp(h\,\mathbf{X}_3) = \mathbf{E}_{(h\,\boldsymbol{e}_z,\mathbf{I})} = \mathbf{E}_{(h\,\boldsymbol{e}_z,\mathbf{I})}\mathbf{E}_{(\mathbf{0},\mathbf{R}^{\boldsymbol{e}_z}_{\alpha})}$. Furthermore, we always have $\mathcal{A}_6\tilde{U}(g) = 0$ for all $g \in SE(3)$. The remaining left-invariant derivatives $\mathcal{A}_i\tilde{U}$, with $i \in \{1,2,4,5\}$, do *not* render α-right-invariant functions since these left-invariant derivatives are dependent on the value of α resp. $\check{\alpha}$. This implies that if one takes higher order derivatives one still needs to take all 6 left-invariant derivatives into account.

As an example, we derive the left-invariant Hessian $\mathcal{H}U = \nabla(\nabla U)$ for α-right-invariant functions where the gradient operator is $\nabla = (\mathcal{A}_1, \mathcal{A}_2, \ldots \mathcal{A}_6)^{\mathrm{T}}$. To this end, we first use the commutator relations to order the numbered left-invariant derivatives such that angular derivative $\mathcal{A}_1$ always appears on the left-side and $\mathcal{A}_6$ always appears on the right-side and subsequently we can use $\mathcal{A}_6 U(g) = 0$ (which implies that $\mathcal{A}_i\mathcal{A}_6 U = 0$ for all i). This yields the following 5×6 Hessian matrix

$$\mathcal{H}\tilde{U} = \nabla(\nabla\tilde{U}) = \begin{pmatrix} \mathcal{A}_1^2 & \mathcal{A}_1\mathcal{A}_2 & \mathcal{A}_1\mathcal{A}_3 & \mathcal{A}_1\mathcal{A}_4 & \mathcal{A}_1\mathcal{A}_5 - \mathcal{A}_3 & \mathcal{A}_2 \\ \mathcal{A}_1\mathcal{A}_2 & \mathcal{A}_2^2 & \mathcal{A}_2\mathcal{A}_3 & \mathcal{A}_2\mathcal{A}_4 + \mathcal{A}_3 & \mathcal{A}_2\mathcal{A}_5 & -\mathcal{A}_1 \\ \mathcal{A}_1\mathcal{A}_3 & \mathcal{A}_2\mathcal{A}_3 & \mathcal{A}_3^2 & \mathcal{A}_3\mathcal{A}_4 - \mathcal{A}_2 & \mathcal{A}_3\mathcal{A}_5 + \mathcal{A}_1 & 0 \\ \mathcal{A}_1\mathcal{A}_4 & \mathcal{A}_2\mathcal{A}_4 & \mathcal{A}_3\mathcal{A}_4 & \mathcal{A}_4^2 & \mathcal{A}_4\mathcal{A}_5 & \mathcal{A}_5 \\ \mathcal{A}_1\mathcal{A}_5 & \mathcal{A}_2\mathcal{A}_5 & \mathcal{A}_3\mathcal{A}_5 & \mathcal{A}_4\mathcal{A}_5 & \mathcal{A}_5^2 & -\mathcal{A}_4 \end{pmatrix} \tilde{U}. \tag{27}$$

We use finite differences to calculate the left-invariant derivatives on orientation scores with a sampled domain $\mathbb{R}^3 \rtimes S^2$. To get a rotation matrix corresponding to an element of S^2 one can choose an arbitrary rotation matrix with $\mathbf{R} \cdot \boldsymbol{e}_z = \boldsymbol{n}$. For first order centered finite differences one subsequently calculates

$$(\mathcal{A}_i U)(\mathbf{E}_g) \approx \frac{1}{2h} \left(U(\mathbf{E}_g \cdot \exp(h\, \mathbf{X}_i)) - U(\mathbf{E}_g \cdot \exp(-h\, \mathbf{X}_i)) \right). \tag{28}$$

Note that this will require interpolations to be performed, both in the spatial dimensions and on the sphere. One should, however, always ensure that the result of the effective operator is independent on the specific choice of $\mathbf{R}$. To this end, we have the following important relation between the left-invariant derivatives at g_1 and g_2 iff $g_1 = (\boldsymbol{x}, \mathbf{R}_1) \sim g_2 = (\boldsymbol{x}, \mathbf{R}_2)$

$$\nabla \tilde{U}(g_1) = \mathbf{Z}_{\alpha_1 - \alpha_2} \nabla \tilde{U}(g_2), \quad \text{with } \mathbf{Z}_\alpha = \mathbf{R}_\alpha \oplus (\,1\,) \oplus \mathbf{R}_\alpha \oplus (\,1\,), \tag{29}$$

where $\mathbf{Z}_{\alpha_1 - \alpha_2} \in \mathbb{R}^{6\times 6}$ "converts" the left-invariant gradient at g_2 to the left-invariant gradient at g_1, rotation matrix $\mathbf{R}_\alpha$ is given by $\mathbf{R}_\alpha = \left(\begin{smallmatrix} \cos\alpha & -\sin\alpha \\ \sin\alpha & \cos\alpha \end{smallmatrix}\right)$, and the symbol "$\oplus$" denotes direct sum of matrices.

3.2 Estimation of Tangent Vectors in $\mathbb{R}^3 \rtimes S^2$

The *exponential curves* of $SE(3)$ are found by (expressed in matrix form)

$$\gamma_{\boldsymbol{c}}(t) = \exp\left(t \sum_{j=1}^{6} c^j \mathbf{X}_j \right), \tag{30}$$

where $\boldsymbol{c} = (c^1, c^2, \ldots, c^6)$ denotes the $SE(3)$-*tangent vector* components, which are elements of the tangent space at the unity element $\sum_{j=1}^{6} c^j \mathcal{A}_j\big|_e \in T_e(SE(3))$, where we use the isomorphism between the Lie algebra and the left-invariant vector fields at the unity element, i.e. $\mathcal{A}_j\big|_e \leftrightarrow \mathbf{X}_j$.

We aim to estimate the locally best fitting exponential curve (in the previous subsection) at each position $SE(3)$. Therefore, we formulate a minimization problem that minimizes over the "iso-contours" of the left-invariant gradient vector at position g, leading to the optimal tangent vector $\boldsymbol{c}^*$

$$\boldsymbol{c}^*(g) = \arg\min_{\boldsymbol{c}(g)} \left\{ \left\| \frac{\mathrm{d}}{\mathrm{d}t} (\nabla \check{U}(g\, \gamma_{\boldsymbol{c}(g)}(t))) \Big|_{t=0} \right\|_\mu^2 \,\middle|\, \|\boldsymbol{c}(g)\|_\mu = 1 \right\}, \tag{31}$$

where $\|\cdot\|_\mu$ denotes the norm on a vector in tangent space $T_g(SE(3))$ (i.e. the norm at the right side) resp. on a covector in the dual tangent space $T_g^*(SE(3))$. The norm on vectors is defined by $\|\boldsymbol{c}\|_\mu = \sqrt{(\boldsymbol{c}, \boldsymbol{c})_\mu}$ with the inner product $(\boldsymbol{c}, \boldsymbol{c})_\mu = \mu^2 \left(\sum_{j=1}^{3} c^j c^j \right) + \sum_{j=4}^{6} c^j c^j$, where parameter μ ensures that all components of the inner product are dimensionless. The value of the parameter determines how the distance in the spatial dimensions relates to distance in the

orientation dimension. After some elementary math, we find that equation (31) can be expressed as

$$(\mathbf{M}_\mu \mathcal{H} U \mathbf{M}_\mu)^{\mathrm{T}} (\mathbf{M}_\mu \mathcal{H} U \mathbf{M}_\mu)\, \tilde{\boldsymbol{c}}^* = \lambda\, \tilde{\boldsymbol{c}}^*, \tag{32}$$

where $\mathbf{M}_\mu = \mathrm{diag}(1/\mu, 1/\mu, 1/\mu, 1, 1, 1)$ and $\tilde{\boldsymbol{c}}^* = \mathbf{M}_\mu^{-1} \boldsymbol{c}^*$. This amounts to eigensystem analysis of the symmetric 6×6 matrix $(\mathbf{M}_\mu \mathcal{H} U \mathbf{M}_\mu)^{\mathrm{T}} (\mathbf{M}_\mu \mathcal{H} U \mathbf{M}_\mu)$, where one of the three eigenvectors gives $\tilde{\boldsymbol{c}}^*$. The eigenvector with the smallest corresponding eigenvalue is selected as tangent vector $\tilde{\boldsymbol{c}}^*$, and the desired tangent vector $\boldsymbol{c}^*$ is then given by $\boldsymbol{c}^* = \mathbf{M}_\mu \tilde{\boldsymbol{c}}^*$.

Once the local tangent vector is found, it is of interest to obtain a measure for *orientation confidence*, which can be used for controlling the anisotropy factor of an adaptive diffusion process, as described for 2D in [2,3]. Such measure can be obtained by calculating the Laplacian in the five-dimensional (considering the full $SE(3)$) hyperplane orthogonal to the estimated tangent vector.

4 Diffusion on 3D Orientation Scores

The general left-invariant diffusion equation on $SE(3)$ is given by

$$\begin{cases} \partial_t W(g,t) = \nabla \cdot \mathbf{D} \nabla W(g,t) = \left(\sum_{i=1}^{6} \sum_{j=1}^{6} \mathcal{A}_j D_{ij} \mathcal{A}_i \right) W(g,t), \\ \partial_t W(g,0) = U(g), \end{cases} \tag{33}$$

where $W(\cdot,t)$ represents the diffused orientation score at time t. This equation generates the diffusion scale space on the 3D Euclidean motion group $SE(3)$.

Next, we will derive which types of diffusions on $SE(3)$ preserve the α-right-invariance of an α-right-invariant input function $\tilde{W}(g,0) = \tilde{U}(g)$. In that case, the right-hand side of (33) becomes, using (29)

$$\nabla \cdot \mathbf{D}(g_1) \nabla \tilde{W}(g_1) = \nabla \cdot \mathbf{Z}_{\alpha_1-\alpha_2}^{\mathrm{T}} \mathbf{D}(g_1) \mathbf{Z}_{\alpha_1-\alpha_2} \nabla \tilde{W}(g_2) = \nabla \cdot \mathbf{D}(g_2) \nabla \tilde{W}(g_2), \tag{34}$$

which shows that diffusion is only *valid* (i.e., α-right-invariance-preserving) if

$$\mathbf{D}(g_1) = \mathbf{Z}_{\alpha_1-\alpha_2} \mathbf{D}(g_2) \mathbf{Z}_{\alpha_1-\alpha_2}^{\mathrm{T}}, \quad \text{for all } g_1 \sim g_2. \tag{35}$$

Next, we separately consider *constant diffusion* (diffusion tensor $\mathbf{D}$ is constant for all $g \in SE(3)$) and adaptive diffusions (diffusion tensor $\mathbf{D}$ varies).

Linear and Constant Diffusion: Suppose $\mathbf{D}$ is an arbitrary diffusion tensor, which is not necessarily valid, one can always make it valid by taking the α-marginal to remove the dependency on α, i.e.

$$\begin{aligned} &\frac{1}{2\pi} \int_0^{2\pi} \nabla \cdot \mathbf{D} \nabla \tilde{W}(g,t) \mathrm{d}\alpha = \frac{1}{2\pi} \int_0^{2\pi} \nabla \cdot \mathbf{Z}_{\alpha-\alpha_0}^{\mathrm{T}} \mathbf{D} \mathbf{Z}_{\alpha-\alpha_0} \nabla \tilde{W}(g_0,t) \mathrm{d}\alpha \\ &= \nabla \cdot \left(\frac{1}{2\pi} \int_0^{2\pi} \mathbf{Z}_{\alpha-\alpha_0}^{\mathrm{T}} \mathbf{D} \mathbf{Z}_{\alpha-\alpha_0} \mathrm{d}\alpha \right) \nabla \tilde{W}(g_0,t) = \nabla \cdot \tilde{\mathbf{D}} \nabla \tilde{W}(g_0,t), \end{aligned} \tag{36}$$

with $\tilde{\mathbf{D}} = \frac{1}{2\pi}\int_0^{2\pi} \mathbf{Z}_\alpha^{\mathrm{T}}\mathbf{D}\mathbf{Z}_\alpha \mathrm{d}\alpha$ and where $g = (\boldsymbol{x}, \mathbf{R}_{(\alpha,\beta,\gamma)})$ and $g_0 = (\boldsymbol{x}, \mathbf{R}_{(\alpha_0,\beta,\gamma)})$. So by considering only diffusion tensors $\tilde{\mathbf{D}}$, α-right-invariance is preserved. All diffusion tensors $\tilde{\mathbf{D}}$ have the form $\tilde{\mathbf{D}} = \mathrm{diag}(A, A, B, C, C, 0)$ (where the sixth value is irrelevant since $\mathcal{A}_6\tilde{U} = 0$). This corresponds to *horizontal*, *zero-curvature* and *zero-torsion*, linear diffusion.

Adaptive Diffusion: In case of adaptive diffusions, both linear and nonlinear, the diffusion above with adaptive A, B, and C is valid as well, since the derivation in (36) can also be applied on an adaptive $\mathbf{D}$. Furthermore, adaptive diffusion with diffusion tensor $\mathbf{D}(g) = \boldsymbol{c}(g)\,\boldsymbol{c}(g)^{\mathrm{T}}$, which can be interpreted as a diffusion process that only diffuses tangent to an exponential curve at each position $g \in SE(3)$ with tangent vector $\boldsymbol{c}(g)$, is a valid diffusion as well. This can be easily seen by observing that $\boldsymbol{c}(g_1) = \mathbf{Z}_{\alpha_1-\alpha_2}\boldsymbol{c}(g_2)$, iff $g_1 \sim g_2$. This yields for the diffusion tensor $\mathbf{D}$

$$\mathbf{D}(g_1) = (\mathbf{Z}_{\alpha_1-\alpha_2}\boldsymbol{c}(g_2))(\mathbf{Z}_{\alpha_1-\alpha_2}\boldsymbol{c}(g_2))^{\mathrm{T}} = \mathbf{Z}_{\alpha_1-\alpha_2}\boldsymbol{c}(g_2)\boldsymbol{c}(g_2)^{\mathrm{T}}\mathbf{Z}_{\alpha_1-\alpha_2}^{\mathrm{T}}, \tag{37}$$

which matches requirement (35).

Furthermore, the sum of two valid diffusion tensors $\mathbf{D}_1 + \mathbf{D}_2$ forms a valid diffusion tensor again since

$$\begin{aligned}\mathbf{D}_1(g_1) + \mathbf{D}_2(g_1) &= \mathbf{Z}_{\alpha_1-\alpha_2}\mathbf{D}_1(g_2)\mathbf{Z}_{\alpha_1-\alpha_2}^{\mathrm{T}} + \mathbf{Z}_{\alpha_1-\alpha_2}\mathbf{D}_2(g_2)\mathbf{Z}_{\alpha_1-\alpha_2}^{\mathrm{T}} \\ &= \mathbf{Z}_{\alpha_1-\alpha_2}(\mathbf{D}_1(g_2) + \mathbf{D}_2(g_2))\mathbf{Z}_{\alpha_1-\alpha_2}^{\mathrm{T}}.\end{aligned} \tag{38}$$

Therefore, in an adaptive setting one can also use a mixture between the between spatially-isotropic diffusion and diffusion along estimated exponential curves, i.e.

$$\mathbf{D}(\boldsymbol{c}, D_{\mathrm{a}}) = (1 - D_{\mathrm{a}})\frac{\mu^2}{\|\boldsymbol{c}\|_\mu^2}\,\boldsymbol{c}\,\boldsymbol{c}^{\mathrm{T}} + D_{\mathrm{a}}\mathrm{diag}(1, 1, 1, \mu^2, \mu^2, \mu^2), \tag{39}$$

where D_{a} is the anisotropy factor. Both D_{a} and $\boldsymbol{c}$ are made dependent on the local structure in the orientation score. This diffusion process is analogous to the nonlinear curvature-adaptive diffusion process on 2D orientation scores that we have proposed in [2, 3].

5 Results

We implemented linear, left-invariant and α-right-invariance-preserving, diffusion on 3D orientation scores with $\tilde{\mathbf{D}} = \mathrm{diag}(A, A, B, C, C, 0)$ using an explicit numerical scheme. The time derivative is taken as a first order forward finite difference. Spatially, we take second order centered finite differences for ∂_x^2, ∂_y^2, and ∂_z^2. In the orientation dimensions we calculate the Laplace operator on the sphere Δ_{S^2} via the spherical harmonic transform, where for stability a small regularization is applied via the spherical harmonic domain as well [11].

In Figure 2 we show a result of the linear $SE(3)$-diffusion process. In these examples an artificial three-dimensional HARDI dataset is created, to which Rician noise [12] is added. Next, we apply two different $SE(3)$-diffusions on

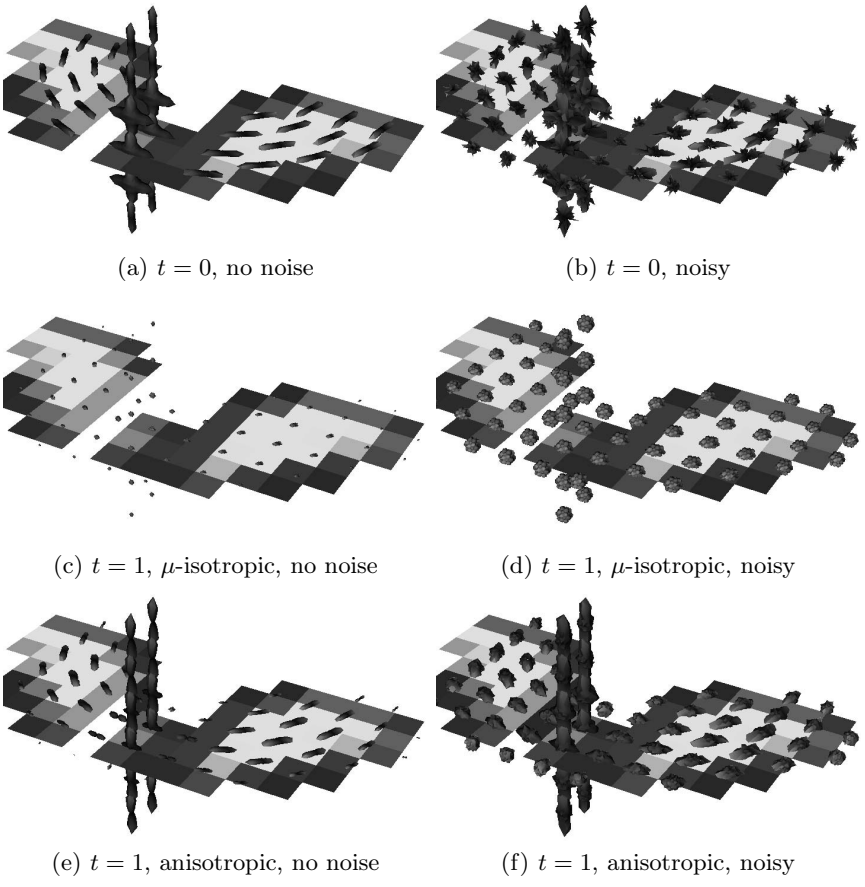

(a) $t = 0$, no noise (b) $t = 0$, noisy

(c) $t = 1$, μ-isotropic, no noise (d) $t = 1$, μ-isotropic, noisy

(e) $t = 1$, anisotropic, no noise (f) $t = 1$, anisotropic, noisy

Fig. 2. Result of $\mathbb{R}^3 \rtimes S^2$-diffusion on an artificial HARDI dataset of two crossing lines where one of the lines is curved, with and without added Rician noise with $\sigma = 0.17$ (signal amplitude 1). Image size: $10 \times 10 \times 10$ spatial and 162 orientations. Parameters of the μ-isotropic diffusion process: $A = B = 1$, $C = 0.01$. Parameters of the anisotropic diffusion process: $A = 0.01$, $B = 1$, $C = 10^{-4}$.

both the noise-free and the noisy dataset. To visualize the result we use an experimental version of the DTI tool, which can visualize HARDI glyphs (recall Figure 1(a)) using the Q-ball visualization method [7]. In the results, all glyphs are scaled equivalently. The μ-isotropic diffusion does not preserve the anisotropy of the glyphs well; especially in the noisy case we observe that we get almost isotropic glyphs. With anisotropic diffusion, the anisotropy of the HARDI glyphs is preserved much better and in the noisy case the noise is clearly reduced. The resulting glyphs are, however, less directed than in the noise-free input image. This would improve when using nonlinear diffusion, or when adding some sort of "thinning" step in the method.

6 Conclusions

In this paper we have shown that we can map all techniques of our previous work on 2D orientation scores to the more complicated case of 3D orientation scores. Some issues require special attention. Especially the fact that we usually have to deal with the coset space $SE(3)/(\mathbf{0} \times \mathrm{stab}(\mathbf{e}_z)) \cong \mathbb{R}^3 \rtimes S^2$ has been emphasized as an important issue. We have shown that we can consider functions $\mathbb{R}^3 \rtimes S^2 \to \mathbb{C}$ as functions on $SE(3)$ which are α-*right-invariant*. The required preservation of α-right-invariance imposed additional constraints on the $SE(3)$-convolution kernel and the allowed types of (non)linear diffusion. The results suggest that even anisotropic *linear* diffusion on $SE(3)$ is a useful way to denoise HARDI data. Future work should include the implementation and evaluation of nonlinear $SE(3)$-diffusion.

References

1. Weickert, J.A.: Coherence-enhancing diffusion filtering. International Journal of Computer Vision 31(2/3), 111–127 (1999)
2. Franken, E., Duits, R., ter Haar Romeny, B.M.: Nonlinear diffusion on the 2D Euclidean motion group. In: Sgallari, F., Murli, A., Paragios, N. (eds.) SSVM 2007. LNCS, vol. 4485, pp. 461–472. Springer, Heidelberg (2007)
3. Franken, E., Duits, R.: Crossing-preserving coherence-enhancing diffusion on invertible orientation scores. International Journal of Computer Vision (IJCV) (to appear, 2009)
4. Özarslan, E., Mareci, T.H.: Generalized diffusion tensor imaging and analytical relationships between diffusion tensor imaging and high angular resolution imaging. Magnetic Resonance in Medicine 50, 955–965 (2003)
5. Franken, E.: Enhancement of Crossing Elongated Structures in Images. PhD thesis, Eindhoven University of Technology, Department of Biomedical Engineering, Eindhoven, The Netherlands (2008)
6. Özarslan, E., Shepherd, T.M., Vemuri, B.C., Blackband, S.J., Mareci, T.H.: Resolution of complex tissue microarchitecture using the diffusion orientation transform (DOT). NeuroImage 31, 1086–1103 (2006)
7. Descoteaux, M., Angelino, E., Fitzgibbons, S., Deriche, R.: Regularized, fast, and robust analytical Q-ball imaging. Magnetic Resonance in Medicine 58(3), 497–510 (2007)
8. Jian, B., Vemuri, B.C., Özarslan, E., Carney, P.R., Mareci, T.H.: A novel tensor distribution model for the diffusion-weighted MR signal. NeuroImage 37, 164–176 (2007)
9. Florack, L.: Codomain scale space and regularization for high angular resolution diffusion imaging. In: IEEE Computer Society Conference on Computer Vision and Pattern Recognition Workshops, 2008. CVPR Workshops 2008, June 2008, pp. 1–6 (2008)
10. Varadarajan, V.: Lie groups, Lie algebras, and their representations. Prentice-Hall, Englewood Cliffs (1974)
11. Kin, G., Sato, M.: Scale space filtering on spherical pattern. In: Proc. 11th international conference on Pattern Recognition, vol. C, pp. 638–641 (1992)
12. Macovski, A.: Noise in MRI. Magnetic Resonance in Medicine 36(3), 494–497 (1996)